Investigations on laser beam welding of hard-to-weld

Aluminum alloys for application in battery housings

Doc.IV-1503-2022

B. Kessler [1*], D. Dittrich [1], R. Strohbach [1], A. Jahn[1]

[1] *Fraunhofer Institute for Material and Beam Technology IWS Dresden, Germany*

[*] Email: benjamin.kessler@iws.fraunhofer.de

Introduction

Aluminum is becoming increasingly important in automotive vehicle construction. On the one hand, its use leads to a reduction in vehicle weight, and on the other hand it offers advantages over fiber composites in terms of recycling, i.e. reusability. Die-casting alloys are used when complex components are required at low costs [TES19]. Furthermore, the use of high-strength wrought aluminum alloys (6XXX and 7XXX) is increasing in crash-relevant structures, for example the battery housings [Has21]. However, during laser beam welding, a high volume of pores and blowouts (die-casting alloys, Fig. 1 a)) and appearance of hot cracks (high-strength wrought alloys, Fig.1 b)) and distortion are often observed [Dit19]. One solution is the application of dynamic beam shaping during, which significantly affects melt pool dynamics as well as cooling behavior and in this way can reduce both weld irregularities [Bör21] and the general use of laser beam welding to reduce the heat input and the result is a minimization of distortion and the appearance of hot cracks.

The object of this paper is to demonstrate the potential of laser beam welding to prevent pores and or hot cracks on technically relevant aluminum alloys at various weld joints for automotive applications in battery housings (Fig.1 a). Laser beam welding is to be the key tool for achieving the high achievable lightweight design potential through the use of aluminum. The weld seams must be able to withstand the very high loads in the event of a crash, static (the battery's own weight) and fatigue as well as sealing.

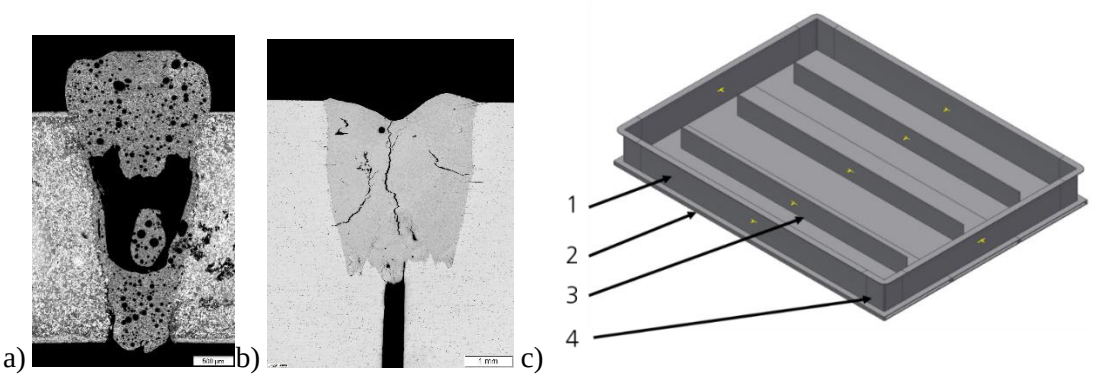

Figure 1: a) Battery housing with side profiles (1), bottom plate (2), profiles to increase stiffness (3), and die-cast nodes (4); b) Reference welding of aluminum die-casting AlSi9MnMoZr by using a static laser beam; c) Reference welding EN AW-6082 T6 with significant hot cracking

1 Experimental Procedure

Technical relevance in the production of battery housing for automotive applications is primarily given to 6XXX alloys in accordance with DIN EN 573-3:2019-10. In the scope of the experiments, different aluminum die-cast and wrought alloys were joined in butt and T-joints with lasers (see Table 1).

Table 1: Aluminum alloys used Alloys

Standard or manufacturer designation	Chemical designation	Standard/ Manufacturer	Wall thickness in mm
Die-cast Alloy			
EN AW-6063	EN AW-AlMg0,7Si	DIN EN 573-3:2019-10	3 and 5
EN AW-6082	EN AW-AlSi1MgMn	DIN EN 573-3:2019-10	3 and 5
Wrought Alloys			
EN AC-43500	EN AC-AlSi10MnMg	DIN EN 1706:2021-10	3 and 5
Castasil®-37	AlSi9MnMoZr	Rheinfelden Alloys GmbH	3

1.1 Experimental Set-up of the Butt Joint Welding

The welding experiments on the butt joints were carried out with high-frequency oscillation of the laser beam to reduce the amount of pores in the weld. A fiber laser of the type IPG YLS 5000-SM with a maximum beam power of 5 kW was used. The beam oscillation was realized with a galvanometer scanner of the type Scanlab weldWeld. The focal diameter was 38 µm. The oscillation parameters were chosen so that a circle with a diameter of 0.3 mm and a frequency of 4 kHz dynamically influenced the molten bath. Argon gas was used to protect the weld pool from oxidation. The weld specimens were clamped pneumatically. The experimental setup can be found in Figure 3 a). The material combinations investigated can be found in Table 2.

Table 2: Material Combinations for Butt joints

Combination	Material 1	Material 2	Wall thickness in mm
1	EN AW-6082 T6	EN AC-43500 F	3
2	AlSi9MnMoZr	AlSi9MnMoZr	3
3	EN AW-6063 T6	EN AW-6063 T6	3
4	EN AW-6063 T6	EN AW-6082 T6	3
5	EN AW-6063 T6	EN AC-43500 F	3
6	EN AW-6063 T6	EN AW-6063 T6	5
7	EN AW-6063 T6	EN AW-6082 T6	5
8	EN AC-43500 F	EN AW-6063 T6	5
9	EN AC-43500 F	EN AW-6082 T6	5
10	EN AW-6082 T6	EN AW-6082 T6	5

1.2 Experimental Set-up of the T-Joint Welding

The fillet welds were realized using a special welding technology which was developed for aviation industry to join skin sheets and stringers together in order to save weight. Figure 2 schematically shows the clamping of the profile/ stringer and the arrangement of the welding heads, which is designed in such a way that both fillet welds are produced simultaneously at the T-joint. This creates a molten pool and subsequently a symmetrical heat input, which shrinks the distortion to a minimum.

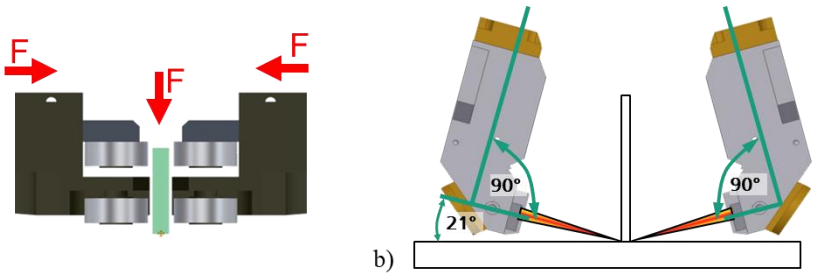

Figure 2: a) Schematic illustration of the profile clamping; b) Schematic illustration of the welding head configuration during welding

The welding tests in the T-joint to produce fillet welds were realized with fiber lasers (IPG - YLS 4000 S2T and nLight - alta prime 4000) and the optical beam shaping was designed to produce focus diameters of 150 µm in each case. The main difference compared to the welding of the butt joints is, that there was no beam oscillation applied. To ensure high weld seam quality, optical sensors were used to detect the weld groove. To protect the molten metal from oxidation, argon was also used as shielding gas from both sides. In some tests, a wire-shaped filler metal (d=0.8 mm) consisting of AlSi12 was used. Figure 3 b) shows the test setup in the laboratory and the clamping of the bottom plate on a vacuum clamping table. The material combinations investigated can be found in Table 3.

Table 3: Material Combinations for T-Joints

Combination	Bottom plate (6 mm)	Profile (3 mm)	Filler Wire
1	EN AW-6063 T6	EN AW-6063 T6	-
2	EN AW-6063 T6	EN AW-6063 T6	AlSi12 (0,8 mm)
3	EN AW-6063 T6	EN AC-43500 F	-
4	EN AW-6082 T6	EN AW-6082 T6	-
5	EN AW-6082 T6	EN AW-6082 T6	AlSi12 (0,8 mm)
6	EN AW-6082 T6	EN AC-43500 F	-

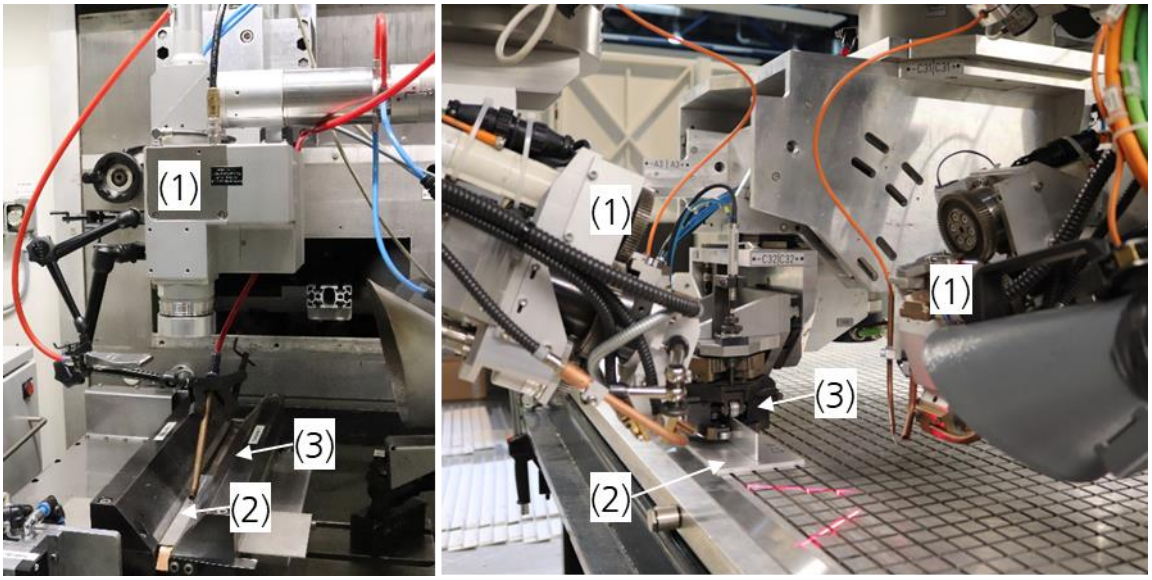

Figure 3: a) Welding of Butt Joints; b) Welding of T-Joints; (1) Welding head, (2) Weld sample, (3) Clamping device

1.3 Tensile test of T-Joints

The tensile test used is not standardized, but is applied in the context of aircraft development [LTH02]. The tests were carried out on a universal testing machine with a maximum load of 50 kN and a test speed of 2 mm/min. The test specimens were taken from the weld specimens as shown in Fig. 4. Three specimens were tested per material combination.

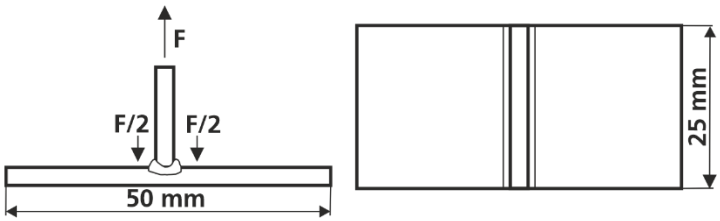

Figure 4: Specimen geometry of the tensile tests

1.4 Fatigue test of Butt joints

The fatigue strength of welded joints made of die-cast aluminum components produced by laser has so far been designed according to the IIW recommendations, but the design parameters having been determined by means of conventionally welded joints produced by arc welding. The aim was therefore to verify their applicability. The fatigue strength was determined on a resonance test machine (Rumul Teststronic) with a test frequency of 88 Hz, a stress ratio of R = 0.1. The maximum number of load cycles was set to $2x10^6$. The specimen where hydraulically clamped and fatigue tested up to failure.

Table 4: Material Combinations for T-Joints

Material 1	Material 2	Wall thickness in mm
EN AW-6082 T6	EN AC-43500	3
AlSi9MnMoZr	AlSi9MnMoZr	3

2 Results of the welding experiments

The following chapter contains the results of the experimental welding process investigations. The welded joints were not subjected to any heat treatment after welding. First, exemplary cross-sections are shown and then selected mechanical properties of the welds are presented.

2.1 Welding of Butt joints

The results of the welding tests are shown in Fig. 5 and Fig. 6 in the form of exemplary cross-sections. The welds of the plates with 3 mm show that the application of the welding technology presented from Dittrich et al. [Dit16] results in quality compliant weld seam quality. Specifically, no weld pool ejections can be observed and the number of voids can be minimized in welded joints with die-cast aluminum alloys compared to the reference welded without beam oscillation in Fig. 1 a). The welded joints between the wrought alloys show positive characteristics with regard to the hot cracks, by the application of beam oscillation and the resulting heat field it is possible to avoid hot-cracks, and this without filler metal.

The cross-sections shown in Figure 6 demonstrate for the first time the application of beam oscillation for plate thicknesses with 5 mm. It can be observed that the welds are still very parallel and thus the effectiveness of beam oscillation and the associated influence on the melt can act over the entire weld depth. Although the welded joints with EN-AC-43500 have pores, these could be reduced to a minimum, so that here, too, sealed and thus quality-compliant welds are produced. The welded joints made of the wrought aluminum alloys (without filler metal) also show no hot cracks and a low number of pores. The cause of the pores is unclear. It is suspected that this is due to inadequate weld preparation in the form

of a saw cut and thus the cleaning of the surfaces was not ideal possible, because oil residues have remained on the surface.

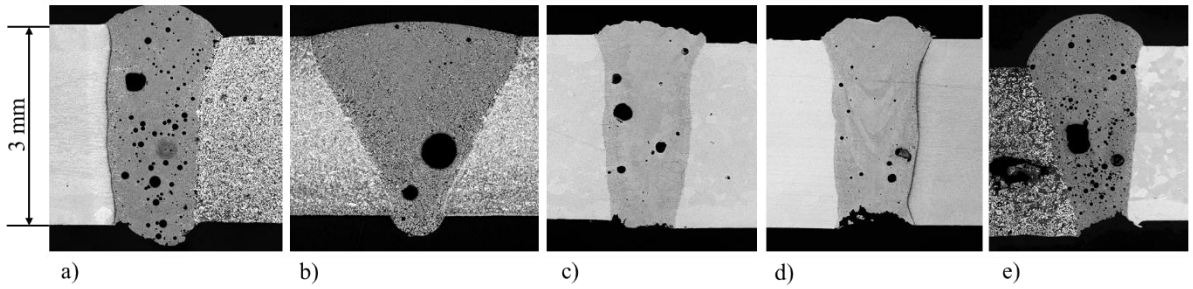

Figure 5: Cross sections of the Butt Joints with 3 mm wall thickness a) EN AW 6082 T6 vs. EN AC-43500; b) AlSi9MnMoZr vs. AlSi9MnMoZr; c) EN AW-6063 T6 vs. EN AW-6063 T6; d) EN AW-6063 T6 vs. EN AW-6082 T6; e) EN AW-6063 T6 vs. EN AC-43500 F

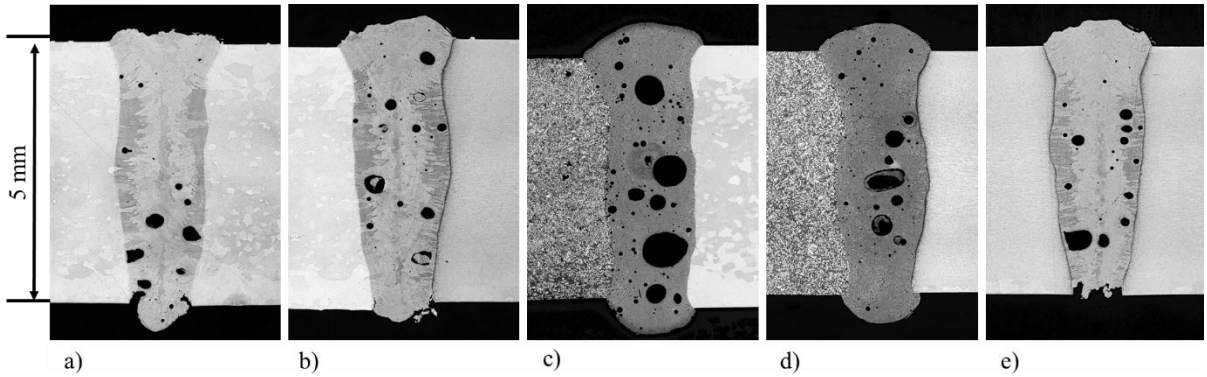

Figure 6: Cross sections of the Butt joints with 5 mm wall thickness a) EN AW-6063 T6 vs. EN AW-6063 T6; b) EN AW-6063 T6 vs. EN AW-6082 T6; c) EN AC-43500 F vs. EN AW-6063 T6; d) EN AC-43500 F vs. EN AW-6082 T6; d) EN AW-6082 T6 vs. EN AW-6082 T6

2.2 Welding of T-Joints

Figure 7 shows the exemplary cross sections of the T-joint welded joints. In contrast to the butt-welded joints, no beam oscillation was used. The welded joints between the wrought alloys in Fig. 7 a) and d) show very significant hot cracking. The use of filler metal in the form of AlSi12 leads to a change in the metallurgy of the weld pool and consequently to a significant reduction in hot cracking in the weld pool. On the basis of the etched sections, however, it can be observed that the mixing with filler material is not effective down to the seam root, and for this reason hot cracks can occasionally be found in the micrograph, particularly in these areas (Fig. 7 b) and e)). The welds between wrought alloy as skin sheet and die-cast alloy as profile (Fig. 7c) and f)) show neither hot cracks nor a very small number of pores for die-cast welds, nor any bonding defects. This is remarkable because the melt pool volume is large and no beam oscillation was used.

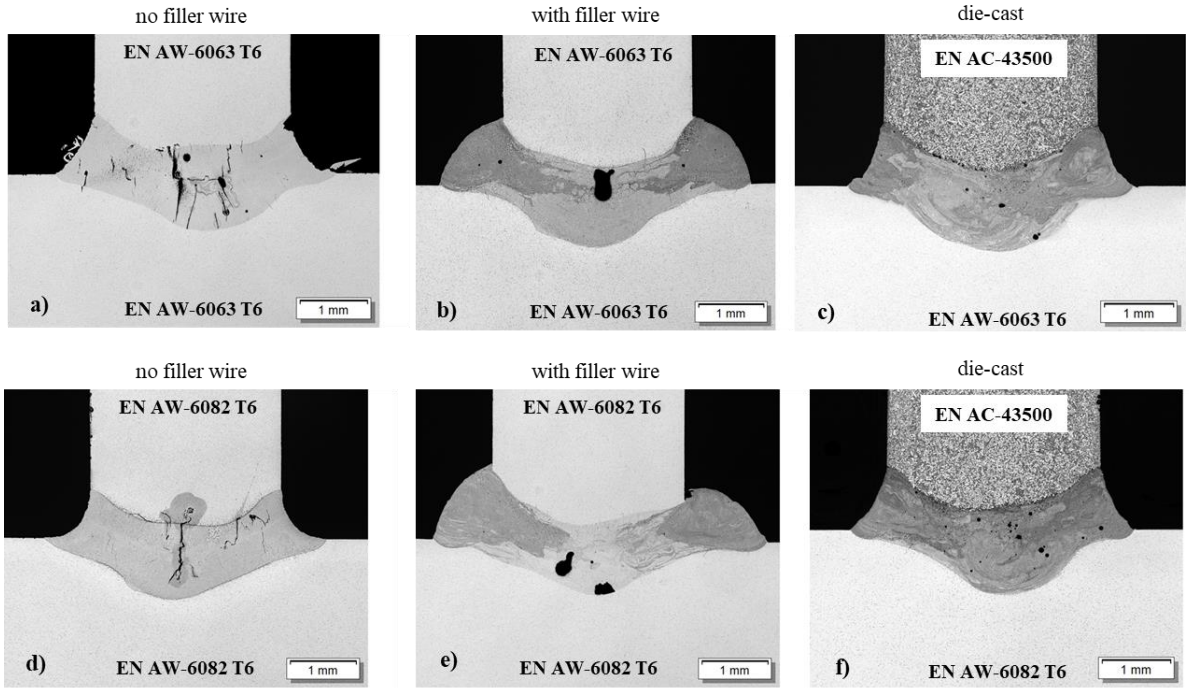

Figure 7: Cross sections of the T-Joints

2.3 Tensile test of T-Joints

Fig. 8 shows the results of the tensile tests of the fillet welded joints shown in Fig. 7. The joints with hot cracks without filler made of EN AW-6063 with EN AW-6063 and EN AW-6082 with EN AW-6082 either have a very low tensile strength or, in the case of the joint between EN AW-6082 with EN AW-6082, could not be tested at all. The use of the filler metal significantly increases the mechanical strength in the case of the combination of EN AW-6063 to values up to 225 N/mm^2 and in the case of EN AW-6082 to 236 N/mm^2. The tensile strengths of the welds with aluminum die-casting also show very good properties and have an averaged tensile strength of 226 N/mm^2 (EN AW-6063 T6 and AlSi10MnMg) and 227 N/mm2 (EN AW-6082 T6 and AlSi10MnMg) and thus the strength properties corresponding to the base material properties according to DIN EN 1706:2021-10 [DIN21].

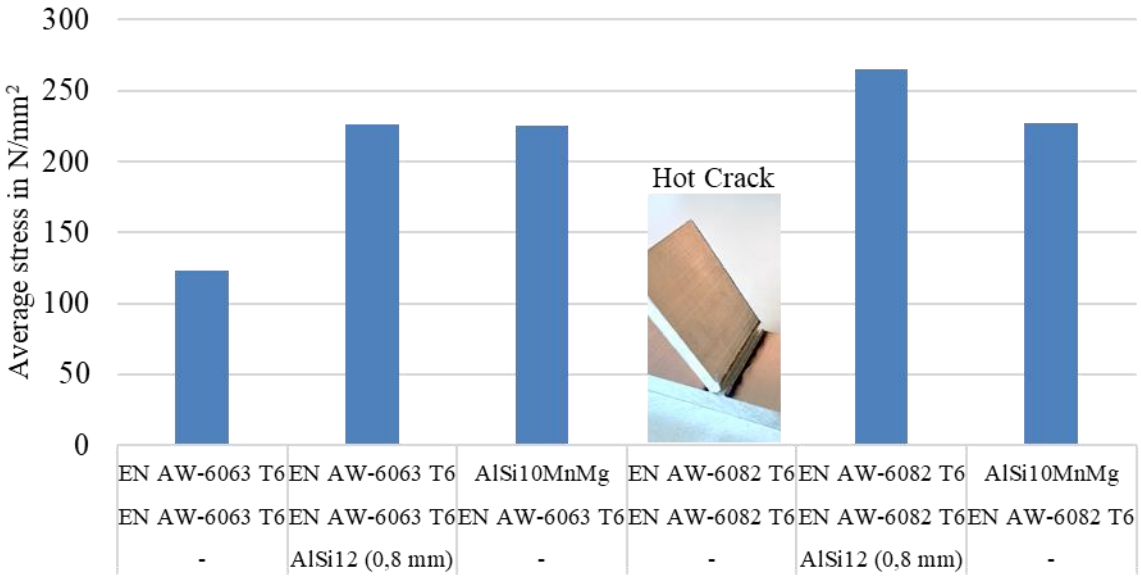

Figure 8: Tensile test of the welded specimens

2.4 Fatigue test of Butt joints

Fig. 9 shows the results of the fatigue tests of the welded joints shown in Fig. 5 a) and b). For classification purposes, the corresponding FAT class has been plotted in the diagram, with the stress ratio R=0.1 according to the conversion recommended from [Hob16]. Fig. 5 does not contain any runs or fractures in the base metal and, accordingly, only specimens that are broken in the weld in the heat affected zone. It can be seen that the fatigue strengths of the welded joints are very good and, especially in the area of high-cycle fatigue strength, can be designed according to the recommendations of the IIW guidelines. In the area of low-cycle fatigue strength, the design according to the applicable code cannot be recommended without doubt, since welded joints made of pure AlSi9MnMoZr in particular are below the FAT28.

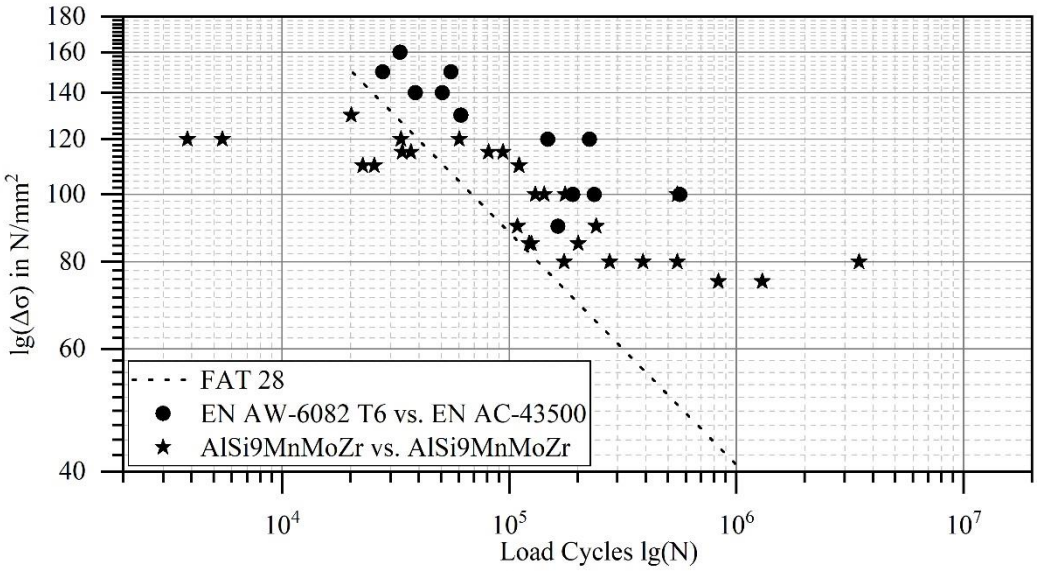

Figure 9: Results of the fatigue tests of the butt joints with 3 mm thickness

3 Summary and Conclusion

Within the scope of the presented investigations, different aluminum alloys were welded together by means of two different laser beam welding processes. The aim was to investigate their applicability for the manufacture of battery housings for use in automotive vehicles. The welding process investigations were able to show that the application of high-frequency beam oscillation can be used, on the one hand, to reduce pores in weld seams even beyond the previously known 3 mm wall thickness (5 mm in this case) and, on the other hand, to minimize or prevent hot cracks in weld seams.

The application of the laser welding process developed for aircraft construction with two lasers producing 2 fillet welds simultaneously also shows promising properties in the cross-section and in the resulting mechanical properties of the welds.

In summary, it can be stated that the investigations show that laser beam welding represents an alternative to the arc welding process being used.

4 Acknowledgements

The results presented were obtained within the framework of the project funded by the Industrial Cooperative Research project with the IGF project no.: 20628 BG and by the funding of the EU within the framework of the European Union's H2020 research and innovation programme under grant agreement No 963580. On behalf of all authors, we would like to thank the funding agencies and all project partners involved.

5 References

[Bör21] Börner, S., Dittrich, D., Mohlau, P., Leyens, C., Garcia-Moreno, F., Kamm, P. H., Neu, T. R., Schlepütz, C. M. (2021): In situ observation with x-ray for tentative exploration of laser beam welding processes for aluminum-based alloys; In: J. Laser Appl. 33, 012026 (2021)

[DIN21] DIN EN 1706:2021-10: Aluminium and aluminium alloys – Castings – Chemical composition and mechanical properties; English version EN 1706:2020+A1:2021

[Dit11] Dittrich, D.: Verbesserung der Belastbarkeit von Haut-Haut-Schweißverbindungen für metallische Integral-Strukturen; Fraunhofer Verlag, Stuttgart 2012, ISBN: 978-3-8396-0375-8

[Dit16] Dittrich, D.; Standfuß, J., Jahn, A. (2016): Neuartiges Verfahren zum druckdichten Laserstrahlschweißen von Aluminium aus Atmosphären-Druckguss; In: DVS-Berichte Band 327, DVS Media, Düsseldorf

[Has21] Hashimura, T.; Shimoda, Y. (2021): Lightweight and cos-effective battery housing case cncept adapting Alumnium and Steel for Evs, and suitable EASW method for dissimilar metal joining; Battery Systems in Car Body Engineering Conference, 26-27 October2021, Bad Nauheim

[Hob16] Hobbacher A.F. (2016): Recommendations for Fatigue Design of Welded Joints and Components; IIW document IIW-2259-15

ex XIII-2460-13/XV-1440-13; Springer International Publishing AG Switzerland

[LTH02] Luftfahrttechnischen Handbuchs 2022 (LTH); Herausgeber:

[TES19] TESLA (2019): Multi-Directional Unibody Casting Machine for Vehicle Frame and Associated Method; Patent: WO 2019/143496Al